Characterization of *FLOWERING LOCUS T* related genes and their putative gene regulatory network in semi-winter *Brassica napus* cultivar Zhongshaung11

Juanjuan Wang[1], Hao-Ran Zhou[1], Petra Tänzler[1], Na Ding[1], Jing Wang[2], Franziska Turck[1]#

[1]Max Planck Institute for Plant Breeding Research, Carl von Linné Weg 10, 50829 Köln

[2]MOA Key Laboratory of Crop Ecophysiology and Farming System in the Middle Reaches of the Yangtze River, College of Plant Science and Technology, Huazhong Agricultural University, Wuhan, PR China. wangjing@mail.hzau.edu.cn

#author for correspondence turck@mpipz.mpg.de

Franziska Turck (ORCID 0000-0002-4982-5949)

Juanjuan Wang (ORCID 0000-0002-1142-6643)

Hao-Ran Zhou (ORCID 000-0001-5945-2448)

Jing Wang (ORCID 0000-0002-7103-8511)

Na Ding (ORCID 0000-0001-8659-7263)

Petra Tänzler (ORCID 0009-0003-7244-2342)

Abstract

In many species, *FLOWERING LOCUS T* (*FT*)-like genes promote the floral transition by integrating environmental signals, in particular photoperiod, and internal cues. Here we show that *Brassica napus* contains 6 *FT*-like genes and 2 pseudogenes belonging to 3 orthogroups. All *B. napus FT*-like genes induce early flowering when expressed at the shoot apical meristems of *Arabidopsis thaliana ft* mutants, but *BnaFT.C6* and non-orthologous *FT*-like genes do not encode fully functional mobile florigens. In the case of *BnFT.C6*, the functional change is associated with a T to C amino acid change that is restricted to semi-winter accessions. Expression of orthologs of *FT* is photoperiod-dependent and two distal enhancers are conserved; however, the homeologs *BnaFT.A7* and *BnaFT.C6* show rearrangements of DNA motifs binding NF-Y/CO and NF-Y transcriptional activator complexes between the promoter and downstream enhancers. Motif rearrangements

correlate with differences in tissue-specific expression. Furthermore, homeologs with rearranged motifs could not be trans-activated by *B. napus* CO in transient assays although they genes show LD photoperiod-dependent expression. We propose that differential diurnal expression of *NF-Y* genes contributes to the photoperiod-dependent regulation of *B. napus FT* genes.

Key words: FLOWERING LOCUS T, *Brassica napus*, flowering time, transcriptional regulation, CONSTANS, NF-Y

Significance statement

B. napus FT-like genes are a case study for gene retention and retraction after multiple rounds of polyploidisation. Retained *B. napus FT*-like genes show preferred expression in different developmental stages and amino-acid changes that affect florigen function.

Introduction

Flowering is an important growth stage in plants with direct impact on biomass, survival and seed production and hence crucial for crop yield. Flowering is promoted by environmental and developmental signals in angiosperms and based on observations made in the model plant *Arabidopsis thaliana,* the underlying flowering promoting pathways have been categorised as the vernalization, photoperiod, autonomous, gibberellin (GA) and age pathways (Andrés and Coupland, 2012; Teotia and Tang, 2015). A major integrator of flowering cues in *A. thaliana* is *FLOWERING LOCUS T* (*FT*), which plays a pivotal role in the photoperiod pathway but also senses cues from other pathways (Bratzel and Turck, 2015; Takagi *et al.*, 2023). FT acts as a mobile florigen, as it is transcribed in the phloem companion cells of leaves in response to a long day (LD) photoperiod. This subsequently allows FT protein to move as a protein through sieve elements to the shoot apical meristem (SAM), where it associates with the transcription factor FLOWERING LOCUS D (FD). The FT/FD complex directly promotes the expression of genes that switch the developmental program of the SAM from vegetative to reproductive growth (Abe *et al.*, 2005; Wigge *et al.*, 2005; Jaeger and Wigge, 2007).

FT-like genes were shown to promote flowering in many plant species; furthermore, as mobile signals they can also impact inflorescence commitment and architecture, shoot branching, storage organ formation and seed dormancy, underscoring their importance for plant fitness (S., Jin *et al.*, 2021). Many plant species show *FT*-like gene expansion, such as the *FT* paralog *TWIN SISTER OF FT* (*TSF*) in *A. thaliana*, which has diversified in expression but not protein function (Yamaguchi *et al.*, 2005). Functional diversification of paralogs has also been reported; for example, *BvFT2* and *BvFT1* in *Beta vulgaris* (sugar beet) respectively activate and repress flowering, which is crucial to integrate vernalization to flowering regulation in this species (Pin *et al.*, 2010).

Research on the transcriptional regulatory mechanisms of *FT* uncovered a network of activating and repressing transcription factors, epigenetic regulators and cis-acting regulatory elements (Takagi *et al.*, 2023; Bratzel and Turck, 2015). *FT* activation in LD requires the combined input of the proximal promoter and two distal transcriptional enhancers, located at 5.7-kb and 1.6-kb distance up- and down-stream of the structural gene, respectively (Liu *et al.*, 2014; Cao *et al.*, 2014; Adrian *et al.*, 2010; Tiwari *et al.*, 2010; Zicola *et al.*, 2019). *FT* regulatory regions recruit related protein complexes: the canonical ternary eukaryotic CCAAT box binding factors (CBF), also known as NF-Y complexes and related plant-specific NF-Y/CO complexes. NF-Y complexes bind CCAAT motifs and are composed of one of each NF-YB, NF-YC and NF-YA subunits.

In NF-Y/CO complexes, the NF-YA component is replaced with the plant-specific CONSTANS, CONSTANS-like, TOC1 (CCT) domain protein CONSTANS (CO). CCT domains exhibit structural similarity to NF-YA, yet demonstrate direct, high-affinity binding to CCACA in lieu of CCAAT motifs (Wenkel *et al.*, 2006; Gnesutta *et al.*, 2017; Lv *et al.*, 2021).

Photoperiod regulation in plants involves transcriptional and post-transcriptional control of CO. Transcriptional control includes the degradation of CO's repressors, such as CYCLIC DOF FACTOR 1-LIKE (CDFs), by a blue light receptor complex that contains FKF1 and GIGANTEA (GI) (Fornara *et al.*, 2009; Imaizumi *et al.*, 2005; Sawa *et al.*, 2007). CO transcription is repressed in the morning and activated in the late afternoon. CO protein decreases in the night due to CONSTITUTIVE PHOTOMORPHOGENESIS 1 (COP1) and SUPPRESSOR OF PHYA-105 (SPA) 1-4 proteins (Laubinger *et al.*, 2006; Jang *et al.*, 2008), while photoreceptors regulate CO stability throughout the day (Valverde *et al.*, 2004; Yanovsky and Kay, 2002; Posé *et al.*, 2013). This regulation allows CO protein to accumulate at dusk under LD but not short day (SD) photoperiod. Additionally, other transcription factors like PHYTOCHROME INTERACTING FACTORs (PIFs) and CRYPTOCHROME 2-INTERACTING bHLH (CIB) proteins modulate *FT* expression in response to light and temperature (Galvão *et al.*, 2019; Fernández *et al.*, 2016; Kumar *et al.*, 2012; Liu *et al.*, 2013; Liu *et al.*, 2018).

A strong motivation for in-depth studies in genetic model organisms is the potential for translational application to crops. While key pathway integrators are mostly conserved, how these are embedded in gene regulatory networks can diverge even between closely related species. The Brassica genus includes important crops, which diverged from *A. thaliana* 27 million years ago. The genus underwent a genome triplication and differentiated three lineages, designated as type A, B and C genomes (Kagale *et al.*, 2014). Detailed comparison of synteny between and within these genomes revealed the presence of a least fragmented (LF) genome and two genomes that were mildly (MF1) or mostly fragmented (MF2) with rearrangements often resulting in gene loss (Parkin *et al.*, 2005; Cheng *et al.*, 2013). Hybrids between Brassica lineages were strongly favoured by early farmers in their selection of crops. The most important, *Brassica napus* (AACC, 2n=38) is mostly grown as oilseed rape (canola) and originated around 7,500 years ago through hybridization between the diploid progenitors *Brassica rapa* (AA, 2n=20) and *Brassica oleracea* (CC, 2n=18), probably in the Mediterranean region (Wu *et al.*, 2019; Chalhoub, 2014; Lu *et al.*, 2019). The global *B. napus* gene pool has undergone several post-domestication ecogeographic radiations, which provided the origin of three cultivars according to their vernalization requirements (Zou *et al.*, 2019). Winter rapeseed is mainly found in Europe

108 and requires a prolonged period of low temperatures to transit from vegetative to reproductive
109 growth; semi-winter rapeseed, mainly produced in China, can initiate flowering after a shorter
110 vernalization period; and spring rapeseed, which presents a wide distribution in Northern
111 Europe, Canada, and Australia, can flower and reproduce without vernalization.

112 Previous studies have shown that gene groups involved in flowering regulation in *A. thaliana*
113 show both expansion and retraction in *B. napus*, indicating that purifying and diversifying
114 selection takes place. In the case of *FT*, six or seven homologs were identified, depending on
115 study and genetic background (Schiessl *et al.*, 2014; Schiessl, 2020). Notably, silencing of a *FT*
116 syntenic *B. napus* gene on chromosome C02 (*BnaFT.C2*) coincided with two TE insertions
117 between the proximal promoter and consequent high levels of cytosine methylation in TE
118 sequences within proximal promoter region (J., Wang *et al.*, 2012). Three *BnaFT* paralogues,
119 designated as *BnaA2.FT*, *BnaC6.FT.a* and *BnaC6.FT.b* were associated with two major QTL
120 clusters for flowering time, in a mapping population from the cross of the winter-type cultivar
121 Tapidor and the semi-winter cultivar NY7 (Wang *et al.*, 2009). Analysis of selective sweeps
122 between spring, semi-winter and winter ecotypes, and GWAS for flowering time confirmed
123 that *BnaFT.A2* (*BnaA02g12130D*) is significantly associated with flowering-time variation (Wu
124 *et al.*, 2019). In addition, EMS-induced mutant alleles of *BnaC6.FT.b* exhibited delayed
125 flowering compared to the control group, while mutants of *BnaC6.FT.a* exhibited flowering
126 patterns akin to the non-mutated parent in winter-type inbred line Express 617 (Guo *et al.*, 2014).
127 Furthermore, loss-of-function mutants in Westar and RNAi lines in Tapidor of *BnaFT*.A2 have
128 smaller leaves, a lower net photosynthetic rate, as well as a substantial delay in flowering time
129 compared to their parents (Jin *et al.*, 2022).

130 Here we present a comparative analysis of six *FT*-like genes encoded by the semi-winter *B.*
131 *napus* cultivar Zhongshaung11 (ZS11).

132 Materials and Methods

133 **Plant material and growth conditions**

134 *A. thaliana* accession Columbia (Col-0) and the *ft-10* T-DNA insertion mutant (GABI-Kat line
135 290E08) were cultivated in a temperature-controlled greenhouse in LD photoperiod (20-24°C,
136 16h light/8h dark) on soil. *B. napus* cultivar ZS11 plants were grown in the greenhouse (20-
137 24°C) for the collection of tissues from different growth stages and in growth chambers (CLF
138 Plant Climatics, AR-95L3X, 60% light intensity (12570 LUX), 75% relative humidity. 22°C)
139 under LD (16 h light /8 h dark) or SD (8 h light /16 h dark) for the collection of leaf material

140 for diurnal transcriptomes. For vernalization, plants were moved to vernalization rooms (4°C,
141 SD).

142 **Identification of *BnaFT* and *NF-Y* homologs in *B. napus***

143 Synteny analysis was performed using the MCscan algorithm (Y., Wang *et al.*, 2012) as
144 implemented in the JCVI toolkit (Tang *et al.*, 2024). Genome sequences and genome annotations
145 for *B. napus* (ZS11.v0) and *Brassica oleracea* var capitata (JZS.v2) (BnPIR;
146 http://cbi.hzau.edu.cn/bnapus) (Song *et al.*, 2020), *Brassica rapa* Z1_v2
147 (https://www.genoscope.cns.fr/externe/plants/data/), *Schrenkiella parvula* v2.2 (Phytozome13;
148 https://phytozome-next.jgi.doe.gov/) and *A. thaliana* Col-0 Araport11 (TAIR;
149 https://www.arabidopsis.org/) were downloaded from the indicated sources. Amino acid
150 sequences of annotated proteins were generated using the scripts of the JCVI toolkit and blasted
151 all against all using the LAST algorithm (Kiełbasa *et al.*, 2011). To identify syntenic genes, 6
152 iterations of comparing all genomes against the *A. thaliana* and *S. parvula* genomes by MCscan
153 were performed.

154 Homologs of FT (AT1G65480) (Supplemental Table 1) and NF-Y proteins (Supplemental
155 Table 2) in *B. napus* var ZS11 were identified using screen criteria of E-value ≤ 1.0E-20,
156 coverage ≥ 95%, identity ≥ 80%. *FT*-like pseudogenes were identified by relaxing the coverage
157 criteria. To include them in the alignment, frameshift mutations and stop codons were corrected
158 according to the output of the Scipio webtool (Hatje *et al.*, 2011). To construct a phylogenetic tree
159 of FT-like proteins, full length protein sequences of FT, TSF, TFL1, BFT and MFT from *A.*
160 *thaliana* were obtained from TAIR database (https://www.*arabidopsis*.org/). Protein
161 alignments were performed with ClustalW and a 60% majority-rule consensus tree was
162 constructed from a bootstrapped (n=1000) neighbor joining (NJ) using MEGA11 (Tamura *et al.*,
163 2021). NF-Y proteins were aligned and visually curated with ClustalW. An maximum-
164 likelihood phylogenetic tree was generated that included *A.thaliana* and *B.napus* homologs of
165 all three NF-Y families for overview.

166 **mVISTA analysis**

167 Genomic sequences including upstream and downstream sequences up to the next flanking
168 genes were submitted to the mVISTA webtool for alignment
169 (https://genome.lbl.gov/vista/mvista/submit.shtml).

170 **Annotation of cis-regulatory motifs at conserved regulatory regions**

171 Sequences identified as aligning to conserved Blocks C, A and E were extracted and re-aligned
172 using ClustalW in MEGA11 (Tamura *et al.*, 2021). Motifs were annotated and plotted using
173 custom scripts in R.

174 **Plasmids construction for complementation and transient expression**

175 The vector *(C+A)-FTpromoter(FTp)-FTcDNA-pGreen* and transgenic *(C+A)-FTp-FTcDNA-*
176 *pGreen/ft-10* plants were described previously (Liu *et al.*, 2014). Full length coding sequences of
177 *BnaFT.A2*, *BnaFT.C2*, *BnaFT.A7*, *BnaFT.C6*, *BnaNFT.A7*, and *BnaCFT.C4* were amplified
178 from ZS11 cDNA using primer pairs as indicated in Supplemental Table 3. PCR products were
179 introduced into *(C+A)-FTp-FTcDNA-pGreen* (Liu *et al.*, 2014) via *Hind*III and *Sac*I restriction
180 enzyme sites to replace the original *FT* CDS on the backbone using NEBuilder® HiFi DNA
181 Assembly Master Mix according manufacturer's instructions (NEB, Frankfurt, Germany).
182 Similarly, the mutant versions of *BnaFT.A7* and *BnaFT.C6*, namely *BnaFT.A7*m and
183 *BnaFT.C6*m, were amplified using mutagenic primers and *(C+A)-FTp-BnaFT.A7-pGreen* and
184 *(C+A)-FTp-BnaFT.C6-pGreen* as the templates.
185 For expression of *FT*-like genes at the shoot apex, the vector *FDp-FD-3xVENUS-pER8* was
186 used as backbone. Full-length coding sequences were amplified with two rounds of PCR to add
187 an N-terminal HA-epitope to the full-length sequence using primers as indicated in
188 Supplemental Table 3. The final PCR products were inserted into vector backbone FDprom-
189 FD3V-pER8 using *Xho*I restriction enzyme sites using NEBuilder® HiFi DNA Assembly
190 Master Mix.
191 For green luciferase (LUC68) reporter vectors, promoters of *BnaFT.A2*, *BnaFT.A7*, *BnaFT.C6*
192 and two fragments of *BnaFT.C2* corresponding to Block C and Block A were amplified from
193 ZS11 gDNA using primer pairs listed in Supplementary Table 3 and introduced via *Sca*I and
194 *Nco*I restriction enzyme sites to replace the *Block A FT* promoter in *BlockA-FTp-LUC68-*
195 *pGreen* using the NEBuilder® HiFi DNA Assembly Master Mix. *BlockA-FTp-LUC68-pGreen,*
196 *5.7Kb-FTp-LUC68-pGreen* vectors were described previously (Adrian *et al.*, 2010). For effector
197 vectors, the cassettes *35Sp-BnaCO.A10, 35Sp-BnaCO.C9*, *35Sp-CO* and *35Sp-H2B* were
198 introduced into the vector *BlockA-FTp-LUC68-pGreen* via restriction enzyme sites *Sca*I and
199 *Sac*I using the NEBuilder® HiFi DNA Assembly Master Mix, to replace *BlockA-FTp-LUC68*.
200 The vector *35Sp-RedLUC-pJAN33* and *35Sp-LUC68-pJAN33* for normalization and filter
201 correction were previously described (Adrian *et al.*, 2010).

202 **Plant transformation**

203 Plasmids were introduced into *Agrobacterium tumefaciens* strain GV3101(pSoup) to transform
204 *ft-10* by floral dipping (Clough and Bent, 1998). Transformants were selected on soil by applying
205 Basta (glufosinate) spray (0.1%) twice for the vectors using *(C+A)-FTp-FTcDNA-pGreen* and
206 on plates supplemented with hygromycin (50 mg/L) for the vectors using *FDp-FD3V-pER8* as
207 the backbone.

208 **Tobacco infiltration and luciferase assay**

209 Suspensions of *A. tumefaciens* GV3101(pSoup) strain carrying the plasmids of interest were
210 mixed according to the experimental design and then infiltrated into the underside of *N.*
211 *benthamiana* leaves as described (Sparkes *et al.*, 2006) with the following adjustments: 10 mM
212 MES and 40 µM acetosyringone were added to the *A. tumefaciens* culture medium, which was
213 then incubated overnight at 28°C. The culture was centrifuged at 4,000 *g* for 15 min and the
214 supernatant was replaced with the infiltration medium to adjust the optical density at 600nm to
215 2.0. Cultures were then placed at room temperature for at least 1 h before being used for
216 infiltration. Infiltrated plants were cultivated overnight in a dark humidified cabinet and then
217 transferred to the greenhouse for 48h. Detection of green luminescent LUC68 and red
218 luminescent RedLUC *in vivo* was performed as described (Adrian *et al.*, 2010). Briefly, leaves
219 were excised, placed on moist filter paper, sprayed with 1mM luciferin dissolved in 0.25%
220 Tween20 and incubated for 1min. Using the digital camera of a LAS4000 device (GE
221 Healthcare), LUC68 and RedLUC signals were integrated sequentially for 2 min through
222 560nm short pass and 610nm long pass camera lens filters, respectively. To calculate the
223 amount of RedLUC activity measured through the green filter and *vice versa*, bombardments
224 with only *35Sp-RedLUC-pJAN33* or *35Sp-LUC68-pJAN33* were performed. The ratios of
225 signals were calculated using a custom script in R based on the Chroma-Luc™ calculator
226 provided by Promega. Bioluminescence signals were quantified from 16bit greyscale images in
227 TIFF format using ImageLab software (Biorad).

228 **RNA extraction, reverse transcription and quantitative reverse transcribed-PCR (qRT-**
229 **PCR)**

230 Total RNA from *B. napus* and *A. thaliana* plants was extracted using the RNeasy Mini Kit
231 (Qiagen, Cat. no. 74104) following manufacturer's instructions. For each sample, 4 µg of total
232 RNA was treated with DNA-free™ Kit (Invitrogen, REF AM1906), and cDNA synthesis was
233 performed with Superscript™ IV reverse transcriptase kit (Invitrogen, REF18090050)
234 following manufacturer's instructions. qRT-PCR was conducted in three technical replicates for

235 each biological replicate using the Bio-Rad CFX384^{TM} system (Bio-Rad), technical replicates
236 were collapsed to their median prior statistical analysis.
237 For the analysis of tissue-specific expression, *B. napus* cultivar ZS11 were cultivated for 4
238 weeks at 22°C in the greenhouse under LD condition, vernalization for 4 weeks at 4°C in SD,
239 and transferred back to the LD greenhouse. Throughout the developmental progression,
240 sequential samplings of three biological replicates occurred at Zeitgeber time 12 (ZT12). Root
241 and leaf 6 were sampled prior to vernalization, leaf 8, paraclade leaf, floral bud, flower and
242 siliques were sampled after vernalization. Material from leaf 8 was also sampled from non-
243 vernalized plants.
244 For diurnal expression analysis, ZS11 was cultivated for four weeks in separate LD or SD
245 growth chambers, followed by an intervening vernalization period of 4 weeks, after which
246 plants were transferred back to the LD or SD chambers, respectively. Leaf 6 was sampled just
247 before plants were transferred to the vernalization and leaf 8 was harvested one week after
248 transfer to LD or SD chambers at 22°C. Biological triplicates were sampled every 4 hours for
249 24 hours. The expression levels of *BnaFT.A2*, *BnaFT.C2*, *BnaFT.A7*, *BnaFT.C6*, *BnaNTF.A7*,
250 *BnaCTF.C4*, *BnaCO.A10*, *BnaCO.C9* and *BnaENTH* in *B. napus* were tested with gene-specific
251 primer pairs that are listed in Supplemental Table 3. Standard curves of each pair of primers
252 were obtained through PCR using gradient-diluted ZS11 genome DNA as the template and Ct
253 values were adjusted using amplification efficiencies prior to using the -ddCt method. The
254 *BnaENTH* gene was used to correct for differences in cDNA concentration, a dilution of
255 genomic DNA was used as common scale for all genes.

256 To measure expression of complementation lines, leaf material was harvested at ZT16 from 14-
257 day old *A. thaliana* plants grown in soil in LD at 22°C in greenhouse conditions. To quantify
258 expression of transgenes in *A. thaliana*, specific primers pairs against *FT*, *BnaNFT.A7*,
259 *BnaCFT.C4* and a common pair for four *BnaFT* genes were titrated against the plasmids used
260 for transformation. A primer pair specific to the phosphinothricin resistance marker (*BAR*) was
261 used to normalize plasmid concentrations, primers against *PROTEIN PHOSPHATASE 2A*
262 (*PP2A*) were used to correct for differences in cDNA amount (see Supplemental Table 3).
263 Expression levels were related to the median *FT* expression in Col-0.

264 **Generation and analysis of RNAseq data**

265 Total RNA from three biological replicates of leaf 8 from 24 h time-courses of vernalized *B.*
266 *napus* var ZS11 plants grown in LD and SD were sent to BGI (Hongkong, China) for library
267 preparation and sequencing using the DNBSEQ platform. Reads were aligned to the reference

268 transcriptome using STAR version 2.7.10b (Dobin *et al.*, 2013) and gene expression was
269 quantified as transcript per million (TPM) using RSEM version 1.3.3 (Li and Dewey, 2011).
270 Diurnally expressed genes were identified using Bioconductor R libraries DESeq2 (Dobin *et al.*,
271 2013) and RAIN (Thaben and Westermark, 2014).

272 Results

273 **The *B. napus* genome carries four functional *FT* orthologous and two *FT* paralogous genes**
274 A protein similarity search against a high-quality assembly of *B. napus* semi-winter cultivar
275 ZS11 (Song *et al.*, 2020) detected eight FT homologs with identity scores above 81%, of which
276 two were annotated as homologs of TSF but covered the query sequence only partially
277 (Supplemental Table 1). A query of the genomic sequence with the Scipio webtool (Hatje *et al.*,
278 2011) confirmed the presence of six complete *FT*-like genes while proteins showing an
279 incomplete overlap are likely pseudo-genes due to presence of frame shifts and/or non-
280 canonical introns in the predicted coding sequence (Supplemental Table 3, Supplemental Figure
281 1).

282 We compared the linearity of lastal hits between *A. thaliana, S. paruvla*, and *B. napus* genomes
283 using the MCscan toolkit (Tang *et al.*, 2008). *S. parvula* is a diploid representative of the
284 Brassicacea lineage II, which includes the genus Brassica. The analysis confirmed that four *FT*
285 syntenic genes are located on chromosomes A02, C02, A07, and C06 (Wang *et al.*, 2009) (Figure
286 1A, Supplemental Data 1). A *TSF* ortholog was present in *S. parvula* but missing at the
287 corresponding syntenic blocks in *B. napus*, indicating gene loss in the genus Brassica rather
288 than a lineage I specific duplication (Figure 1B). On the other hand, *S. parvula* and *B. napus*
289 featured an *FT*-like gene at a novel syntenic position on chromosome A07, for which no
290 correspondence could be found in *A. thaliana* (Figure 1C). This gene is a homeolog of both *FT*-
291 like pseudogenes. We propose the name *NEW SISTERS OF FT AND TSF* (*NFT*) to distinguish
292 them from *FT* or *TSF* orthologous genes. *BnaFT.A7*/*BnaNFT.A7* and *BnaFT.C6*/Pseudo-
293 *BnaNFT.C6* are located near a region showing a large inverted duplication in Chromosomes
294 A07/C06 (Parkin *et al.*, 2005); however juxtaposition with the *FT* and *NFT* syntenic segments
295 showed that the *FT* gene is situated at the margin of the original syntenic fragment, narrowly
296 avoiding the duplication (Supplemental Figure 2). A sixth functional *FT*-like gene was located
297 on chromosome C04 at a position unique to *B. napus* and the C-genome parent *B. oleracea*, but
298 absent from *B. rapa*, *S. parvula* and *A. thaliana* (Figure 1D). We propose the name *C-GENOME*
299 *SISTER OF FT AND TSF* (*CFT*) for this gene.

300 A bootstrapped neighbour-joining phylogenetic tree was constructed from the alignment of six
301 functional FT-like proteins, two frame-corrected pseudogenes and FT homologs from *B. rapa*,
302 *B. oleracea*, *S. parvula, A. lyrata* and *A.thaliana*. TERMINAL FLOWER 1 (TFL1), BROTHER
303 OF FT AND TFL1 (BFT) and MOTHER OF FT AND TFL1 (MFT) were added as outgroups
304 (Figure 1E). In this tree, TSF/*Al*TSF clustered together with TSF from *S. parvula* and NFT/CFT
305 proteins indicating a more recent duplication history for non-*FT* orthologs (Figure 1A).

306 **Six extant *B. napus FT* homologs show divergence in their potential to act as mobile**
307 **florigen**

308 To elucidate the potential of FT-like proteins from *B. napus* to act as mobile florigen, the
309 corresponding cDNAs were stably transformed into the *A. thaliana ft-10* mutant under the
310 control of a modified *FT* promoter (*(C+A)-FTp*) that was previously shown to drive transgene
311 expression in phloem companion cells similar to endogenous *FT* in LD photoperiod (Figure2A)
312 (Liu *et al.*, 2014). First, flowering time of at least 4 independent segregating T2 lines was
313 compared by comparing the median values of total leaves (Supplemental Figure 3A and B).
314 These results indicated two distinct complementation groups with *BnaFT.A2*, *BnaFT.A7* and
315 *BnaFT.C2* complementing *ft-10* with delay of 5 to 10 leaves compared to *FT* control lines while
316 *BnaNFT.A7,BnaCFT.C4* and *BnaFT.C6* transgenic lines flowered almost as late as *ft-10*. In
317 order to exclude that expression differences were the cause of the observed variation in
318 complementation, we quantified transgene expression in T3 lines with single locus insertions
319 (Supplemental Figure 3C and D). Signals were quantified against the plasmids used for
320 transformation to allow the direct comparison of expression levels between genes. Although
321 large variation in transgene expression explained outliers within genotypes, lines within +/- 4-
322 fold expression band compared to *FT* in Col-0 showed no correlation between expression and
323 flowering time (Supplemental Figure 3C and D). The analysis of two representative T2 lines
324 per genotype confirmed the presence of four complementation groups ranging from *FT* showing
325 full complementation, followed by *BnaFT.A2/BnFT.A7/BnaFT.C2*, then
326 *BnaFT.C6/BnaNFT.A7/BnaFT.C4* with increasingly partial complementation and, last, *ft-10*
327 (Figure 2B). In contrast, when *B. napus FT*-like genes were expressed directly in the SAM
328 under the control of the *FD* promoter (*FDp*) (Figure 2A)(Abe *et al.*, 2005), independent T1 lines
329 expressing *FT* or *B. napus FT* homologs flowered earlier than wild type controls, although *FDp-*
330 *BnaCFT.C4* lines flowered slightly later than all other lines (Figure 2C).

331 The florigenic BnaFT.A7 and the non-florigenic BnaFT.C6 of cultivar ZS11 differ at 5 amino-
332 acid residues, of which none correspond to five FT residues (D17, V18, V70, S76, and R83)

333 previously identified as important for intercellular trafficking (Yoo *et al.*, 2013; Endo *et al.*,
334 2018) (Supplemental Figure 4). The carboxy-terminus is important for FT function, which is
335 abolished by the deletion of the last nine amino acid residues (Kim *et al.*, 2016). The presence of
336 a cysteine at the last position of BnaFT.C6 instead of the threonine of BnaFT.A7 alters
337 biochemical properties and could cause covalent protein-protein cross-linking under oxidizing
338 conditions (Figure 2D). Modified protein versions carrying a mutual exchange of the last
339 residue (BnaFT.A7m and BnaFT.C6m) were expressed in *ft-10* under the control of *C+A-FTp*.
340 T1 plants transformed with *BnaFT.A7m* showed a significant delay in flowering compared to
341 *BnaFT.A7* transformed lines (Figure 2E). In contrast, *BnaFT.C6m* T1 plants did not flower
342 earlier than *BnaFT.C6* transformed plants. Taken together, the data indicate that a cysteine as
343 the last amino-acid contributed to a reduced florigen function of BnaFT.C6, but was not the
344 only determinant. Comparison of BnaFT.C6 from different cultivars revealed that the threonine
345 to cysteine change at the last amino-acid position was only found in a subset of semi-winter
346 cultivars (Supplemental Figure 5).

347 **Expression of *FT* homologs across tissues**

348 Although *BnaFT.C6*, *BnaNFT.A7* and *BnaCFT.C4* may not encode fully functional mobile
349 florigens, they induce flowering if transcribed close to the apical meristem. We compared
350 steady-state mRNA levels of *BnaFT*-like genes in different tissues and developmental stages in
351 the cultivar ZS11 grown in LD with and without vernalization (Figure 3). Genomic DNA was
352 used as a common reference point to allow copy-number comparisons of mRNA levels between
353 homologs. Without vernalization, no differences in steady-state mRNA levels were detected
354 between leaf 6 and leaf 8. In the case of vernalized plants, leaf 6 and leaf 8 were fully expanded
355 before and after the plants were moved to and out of the vernalization chamber, respectively.
356 *BnaFT.A7* and *BnaFT.C6* were strongly induced in leaf 8 of vernalized compared to non-
357 vernalized plants, while *BnaFT.A2* was vernalization-responsive but less induced. As
358 previously reported, *BnaFT.C2* was barely expressed, which has been attributed to the presence
359 of several TE insertions at the locus (J., Wang *et al.*, 2012). After vernalization, *BnaFT.A2* was
360 expressed at much lower levels than *BnaFT.A7*/*BnaFT.C6* in leaf 8, but became the highest
361 expressed *FT*-like gene in paraclade leaves. Steady-state mRNA levels were similar for all three
362 *FT* orthologs in floral buds, flowers and developing siliques. In contrast, expression of
363 *BnaFT.C2, BnaNFT.A7* and *BnaCFT.C4* was low throughout development; therefore, these *FT*-
364 like genes are unlikely to play a major regulatory role for flowering regulation or inflorescence
365 development under our test conditions.

366 **Conservation of cis-regulatory regions at *B. napus FT* homologs**

367 Previous reports established that the distal *FT* enhancer Block C is conserved at *FT* orthologs
368 between *B. napus* and *A. thaliana* (J., Wang *et al.*, 2012; Adrian *et al.*, 2010). Here we show
369 that this is also the case for Block E, which is located downstream of the structural gene. *FT*
370 orthologs of *B. oleracea*, *B. rapa* and *S. parvula* showed the presence of all three blocks, while
371 non-orthologous *FT* homologues showed no conservation of the distal blocks and limited
372 conservation at the proximal promoter Block A (Supplementary Figure 6).

373 In *A. thaliana*, *FT* transcription is dependent on the NF-Y/CO-complex, but also requires
374 canonical NF-Y complexes, that contain NF-YA family proteins instead of CO (Wenkel *et al.*,
375 2006; Siriwardana *et al.*, 2016; Kumimoto *et al.*, 2010; Kumimoto *et al.*, 2008). The effect of NF-Y is
376 likely mediated by cognate CCAAT-boxes located at the distal enhancers Block C and Block E
377 (Zicola *et al.*, 2019; Cao *et al.*, 2014; Siriwardana *et al.*, 2016). A CCACA-motif as high-affinity
378 binding site of the CO-complex is found three times at Block A; a CCACT-motif that still binds
379 the CO-complex with fair affinity is found twice (Gnesutta *et al.*, 2017) (Figure 4A). The function
380 of three distinct CCACA-motifs, named P1, P2 and CORE2, has been experimentally validated
381 (Tiwari *et al.*, 2010; Adrian *et al.*, 2010). In *B. napus*, CO-binding motifs P2 and CORE2 are present
382 at *BnaFT.A2/BnaFT.C2,* P1 is a CCACT-motif in *BnaFT.A7*, *BnaFT.A2*, *BnaFT.C2* and *SpFT*,
383 while an additional C to A change creates a CCAAT-motif at the same position in *BnaFT.C6*.
384 A second change from CCACT- to CCAAT-motif is common to *BnaFT.C6*, *BnaFT.A7* and
385 *SpFT*. *BnaFT.C6* contains a third, private CCAAT-motif close to the transcription start site. A
386 recent structural study of the CO-complex with target DNA indicated that only the CACA core
387 of the first motif was involved in protein-DNA interactions (Lv *et al.*, 2021). Two additional
388 CACA-motifs can be identified at Block A of which one is present in all *BnaFT* paralogs and
389 *SpFT*. In sum, CO-binding CCACA-motifs are observed in block A in a decreasing trend from
390 *BnaFT.C6* to *BnaFT.A7*, *SpFT*, *BnaFT.A2/BnaFT.C2* and *FT*, while a trend towards more NF-
391 Y-binding CCAAT-motifs is observed in the opposite order. Notably, the trend to more
392 promoter-located CCAAT-motifs correlated with higher expression levels in leaves.

393 At Block C, an important CCAAT-motif is conserved in all *FT* orthologs (Figure 4B), but at
394 the downstream enhancer Block E, *SpFT*, *BnaFT.C6* and *BnaFT.A7* share a CCACA-motif that
395 is not present at the other genes; furthermore, *BnaFTA7* and *BnaFTC6* have evolved two
396 additional CCACA sites as candidates for binding a CO-complex (Figure 4C). In contrast, the
397 first CCAAT motif has been lost at these homeologs.

398 To test whether the variation in *cis*-motifs at *B. napus FT* promoters had an impact on gene
399 activation by CO, we cloned upstream sequence of *FT* and *B. napus* orthologs to a binary

400 reporter vector with green shifted Luciferase that allowed us to test transactivation by *B. napus*
401 CO homologs in transiently infiltrated tobacco leaves using a co-infiltrated red shifted
402 luciferase for normalization. The distance between regulatory blocks differs greatly in *B.napus*
403 and we could not amplify the 21 Kb promoter region of *BnaFT.C2;* however, we could amplify
404 and fuse the regions corresponding to Block C and Block A (*C+A-BnaFT.C2*) (Figure 4D). We
405 tested ca. 12Kb long *BnaFT.A2* and *BnAFT.A7* promoters, 2Kb long *BnaFT.C6* and *C+A-*
406 *BnaFT.C2* promoters and a 5.7Kb long *FT* promoter for reporter gene induction in response to
407 *CO*, *BnaCO.A10* and *BnaCO.C9* controlled by the *CaMV 35S* promoter. We found that
408 promoters of *FT*, *BnaFT.A2* and *C+A-BnaFT.C2* were activated in the presence of COs while
409 the homeolog pair *BnaFT.A7/BnaFT.C6* was not or significantly less induced (Figure 4E).
410 In sum, *BnaFT.A2* and *C+A-BnaFT.C2*, which show conservation of putative CO binding
411 CCACA-motifs at the proximal promoter are responsive to CO homologs in transient assays,
412 while homeologs *BnaFT.A7/BnaFT.C6* respond poorly to transactivation, which corresponds
413 to the absence of conserved CO- binding motifs.

414 **Diurnal expression pattern of *B. napus FT* homologs in response to photoperiod and**
415 **vernalization**

416 Since the homeologs Bna*FT.A2/BnaFT.C2* and *BnaFT.A7/BnaFT.C6* showed remarkable
417 differences in the distribution of cis motifs across regulatory blocks, we compared their
418 transcript levels across time-series of plants grown in SD and LD photoperiod both before and
419 after vernalization. The analysis confirmed that *BnaFT.A2*, *BnaFT.A7* and *BnaFT.C6* respond
420 to vernalization; furthermore, expression was induced by LD versus SD conditions, with a
421 strong synergism between LD and vernalization signals (Figure 5). The expression of
422 *BnaFT.C2* was low (approximately 20 and 100 times less than *BnaFT.A2* and *BnaFT.C6,*
423 respectively) but essentially followed the same induction pattern. In the case of non-*FT*
424 orthologs, *BnaCFT.C4* mirrored the vernalization response and the diurnal expression pattern
425 of *BnaFT* genes, at a level 10 times lower than even *BnaFT.C2*. *BnaNFT.A7* was only notably
426 expressed at the beginning of LDs before vernalization. Overall, apart from *BnaNFT.A7*, *FT*-
427 like genes shared an expression minimum at ZT8 and high expression throughout the night until
428 the next morning (Figure 5 A and B).

429 **Photoperiod-dependent regulation of putative *B. napus FT* activators**

430 Differences in the arrangement of cis-motif for NF-Y/CO- and NF-Y complexes between
431 regulatory regions did not abolish the dependence of *BnaFT* genes on LD photoperiod. In *A.*
432 *thaliana*, the accumulation of CO protein in the second half of long days largely explains LD

433 dependency of *FT* expression, but it is not yet addressed if this model applies to other
434 Brassicaceae. We measured steady-state transcript levels of *BnaCO.A10* and *BnaCO.C9* in
435 leaves throughout SD and LDs before and after vernalization (Figure 5C). As previously
436 described, *BnaCO.C9* mRNA accumulated at higher levels than *BnaCO.A10* (Q., Jin *et al.*, 2021).
437 Both genes showed higher expression in LD vs SD, with similar trends before and after
438 vernalization. As observed for *BnaFT*-like genes, transcript levels of both *BnaCO* genes showed
439 a trough at ZT8 in LD. For *BnaCO.A10,* the general pattern of transcript accumulation was
440 similar in SD and LD, showing an increase during the dark and at dawn. For *BnaCO.C9*, steady-
441 state levels declined 8 h after the onset of the dark period in SD corresponding to the onset of
442 dark in LD, but transcript levels continued to increase in LD during the dark period. Under the
443 assumption that CO proteins in *B. napus* require light for stabilization, only *BnaCO.A10*
444 transcripts accumulating in the morning would contribute to a NF-Y/CO complex in the
445 morning in SD, while both COs could contribute to early morning and late afternoon NF-Y/CO
446 complexes in LD.
447 To assess whether NF-Y components could also limit *FT* gene expression in *B. napus*, we
448 generated RNAseq libraries of a diurnal time-series of vernalized ZS11 plants grown in LD and
449 SD photoperiod. Of the annotated 95560 nuclear *B. napus* genes, 47198 were considered as
450 expressed (at least 25 transcripts per million (TPM) summed across all samples) (Supplemental
451 Data 2). After applying the Rhythmicity Analysis Incorporating non-Parametric methods
452 (RAIN) pipeline with a FDR <0.05, 33714 genes (71,4%) scored as diurnally expressed, with
453 a slightly higher number in SD vs LD (29596 vs 21757). Most genes were detected as diurnally
454 expressed in both photoperiods (52.3%), but more genes were SD- than LD-specific (35.5% vs
455 12.2%, respectively) (Figure 6A, Supplemental Data 3).
456 We re-annotated *B. napus* NF-Y genes based on synteny to *A. thaliana* homologs and removed
457 four genes that were annotated as NF-Y genes but that likely encoded by pseudogenes due to a
458 partial protein prediction and/or frame-shift mutations (Supplemental Table 4, Supplemental
459 Figure 6). We found that 78 of 106 NF-Y genes were expressed, of which 55 showed diurnal
460 changes in their transcript levels. The fraction of diurnally expressed NF-Y genes is as expected
461 and although a slightly greater than expected number of NF-Y genes showed LD-specific
462 rhythmicity, this was not statistically significant (Figure 6B). Hierarchical clustering of
463 diurnally expressed *B. napus* NF-Y genes based on their transcript accumulation patterns
464 (normalized across all samples) identified 3 major clades (Figure 6C). A clade containing 29
465 NF-Y genes was expressed at higher level in LD versus SD and showed a marked peak of
466 expression in the critical afternoon light period from ZT12 to ZT16 in LD. The clade also

467 included *BnaFT* and CO genes that had been added to the clustering analysis; however,
468 expression of these genes extended to the dark phase and/or showed later peak values than
469 ZT16.
470 In *A. thaliana*, NF-Y paralogs with a critical role in *FT* expression were identified by their
471 phloem-specific expression and subsequently tested by reverse genetic approaches (Kumimoto
472 *et al.*, 2010; Siriwardana *et al.*, 2016; Kumimoto *et al.*, 2008). Although the tissue-specific expression
473 pattern of NF-Y genes in *B. napus* is unknown, it is noteworthy that 4 of 4 NF-YB2 homologs,
474 4 of 5 NF-YC9 homologs and 2 of 3 NF-YA2 homologs, all orthologs of photoperiod-
475 responsive NF-Ys, are part of the expression cluster with an LD-specific peak at ZT16. *B. napus*
476 homeologs are likely to act redundantly and we therefore prepared cumulative plots that
477 consider the expression of all *B. napus* NF-YB2, NF-YC9 and NF-YA2 genes (Figure 6 D-F).
478 If the sum of the expression of all homeologs is considered, a marked peak of expression at
479 ZT16 in LD and an overall higher expression in LD vs SD was detected. In sum, NF-Y genes
480 that are candidates for photoperiod-dependent induction of *FT*-like genes could strongly
481 promote *FT* expression at the end of LD.

482 # Discussion

483 Land plants share a recurrent history of whole genome duplications (WGD) through
484 polyploidisation and subsequent retraction of the coding genome (Panchy *et al.*, 2016). In some
485 cases, homeologs may be retained if increased gene dosage of redundant genes confers a fitness
486 advantage, but more often retention is linked to partial redundancy either through the evolution
487 of divergent expression patterns or through preferred interactions with other protein partners.
488 *B. napus* is a particularly rewarding case for study, combining two paleontological events with
489 different outcomes with a recent hybridisation event that has been partially shaped by human
490 selection for crop traits (Lu *et al.*, 2019; Parkin *et al.*, 2005).
491 Analysis of the genome of the genus Brassica suggests that one of the paleo-duplications
492 resulted in unequal retention of homeologs, while for the second event, two fairly co-linear
493 genomes can still be recognized (Parkin *et al.*, 2005). Only two *FT* syntenic genes are conserved
494 per Brassica genome lineage, indicating a loss of the copy of the weaker genome from the first
495 polyploidisation event. *NFT* and *CFT* are not survivors of the weak genome as syntenic copies
496 can be detected in *S. paruvula,* a sister genus of *Brassica* that did not undergo whole genome
497 duplication (Figure 1) (Cheng *et al.*, 2012). Differences in expression may have contributed to the
498 maintenance of both *FT* paralogs. In the case of the Brassica A genome, both paralogs are
499 expressed; however, expression seems specialised as *BnaFT.A7* and *BnaFT.A2* show higher

500 expression in rosette and paraclade leaves, respectively (Figure 3). In the case of the C-genome,
501 *BnaFT.C2* is barely expressed, probably due to the presence of TE insertions that are common
502 to *B. napus* but not to all *B. oleracea* varieties (J., Wang *et al.*, 2012). Since *BnaFT.C2* encodes a
503 fully functional florigen (Figure 2), the presence of a second *FT*, even if only marginally
504 expressed, may be advantageous under certain conditions and therefore retained. Similarly,
505 circumstances causing the induction of *BnaNFT.C6* and *BnaCFT.C4* could influence flowering
506 and convey an advantage; however, *BnaNFT.C6* homeologs have not survived as functional
507 genes (Figure 1). Similarly, *BnaFT.C6*, the second *FT* of the C-genome may be impaired or at
508 least attenuated for its florigen function (Figure 2). The amino acid change from threonine to
509 cysteine, which contributed to the reduced systemic function, is not found in all *B. napus*
510 accessions (Supplemental Figure 4). Further studies are required to clarify whether the mutation
511 can be linked to a flowering QTL. In the case of the semi-winter *B. napus* variant ZS11, both
512 *FT* genes originating from the C-genome seem compromised in their function.
513 *A. thaliana FT* regulation depends on an intricate interplay of two distal enhancers with an
514 accessible chromatin structure and a proximal promoter that is inaccessible (Zicola *et al.*, 2019).
515 Binding of NF-Y complexes to distal enhancers is thought to somehow increase the probability
516 of NF-Y/CO to bind to the proximal promoter and increase expression; how NF-Y/CO binding
517 is mechanistically linked the induction of transcription is currently unknown. Although the cis-
518 regulatory Blocks were found as conserved at all *B. napus FT* genes, the shift from NF-Y/CO
519 to NF-Y binding sites at the proximal promoter was unexpected and raises a couple of questions
520 (Figure 4). First, can binding of NF-Y simply replace NF-Y/CO causing similar effects leading
521 to the induction of transcripts? Second, if NF-Y binding is sufficient to induce expression, what
522 limits induction of BnaFTA7/BnaFTC6 to LD? Here, we propose that transcriptional regulation
523 of NF-Y genes may contribute to photoperiod control (Figure 6). Alternatively, *B.napus* CO
524 proteins as part of a NF-Y/CO complex binding to the distal enhancer could contribute as
525 limiting factors, but how it could do so is not obvious. Gnesutta et al. determined the binding
526 preferences of the NF-Y/CO complex to DNA (Gnesutta *et al.*, 2017). The preferred binding motif
527 for NF-Y/CO (CCACA) is two nucleotide edits away from the CCAAT motif. We found that
528 replacement of motifs happened at conserved in the proximal promoter and propose that an
529 intermediate CCACT motif that can still be bound (or already be bound) by NF-Y/CO served
530 as stepping stone during the motif change (Figure 4).
531 In sum, *B. napus* photoperiod dependent regulation of *FT*-like genes is a case study for the
532 consequence of gene duplications, indicating gene retraction through loss-of-function,

533 homeolog retention partially explained by differences transcriptional regulation and possibly
534 variation between cultivated varieties due to changes in protein function.
535

536 Data availability

537 RNAseq datasets generated and analysed in the current study are available at the European
538 Nucleotide archive under the accession number project accession number PRJEB82128.

539 Acknowledgements

540 JW is grateful for the funding from the Chinese Scholarship Council. FT and HZ are supported
541 by core funding from the Max Planck Society.

542 Competing interests

543 None declared.

544 Author contributions

545 JJW and FT outlined, created figures and wrote the manuscript outline. JJW and PT performed
546 all experimental work, ND provided the FDp-FT-pER8 construct and helped with cloning, FT
547 and HRZ contributed with guidance and critical discussion. JJW and FT performed all data
548 analysis. JJW, FT, HRZ and JW were involved in revising the manuscript.

549

550 # References

551

552 **Abe, M., Kobayashi, Y., Yamamoto, S., et al.** (2005) FD, a bZIP protein mediating signals
553 from the floral pathway integrator FT at the shoot apex. *Science*, **309**, 1052–1056.

554 **Adrian, J., Farrona, S., Reimer, J.J., Albani, M.C., Coupland, G. and Turck, F.** (2010)
555 cis-Regulatory elements and chromatin state coordinately control temporal and spatial
556 expression of FLOWERING LOCUS T in Arabidopsis. *Plant Cell*, **22**, 1425–1440.

557 **Andrés, F. and Coupland, G.** (2012) The genetic basis of flowering responses to seasonal
558 cues. *Nat. Rev. Genet.*, **13**, 627–639.

559 **Bratzel, F. and Turck, F.** (2015) Molecular memories in the regulation of seasonal
560 flowering: from competence to cessation. *Genome Biol.*, **16**, 192.

561 **Cao, S., Kumimoto, R.W., Gnesutta, N., Calogero, A.M., Mantovani, R. and Holt, B.F.**
562 (2014) A distal CCAAT/NUCLEAR FACTOR Y complex promotes chromatin looping at
563 the FLOWERING LOCUS T promoter and regulates the timing of flowering in
564 Arabidopsis. *Plant Cell*, **26**, 1009–1017.

565 **Chalhoub, B.** (2014) Early allopolyploid evolution in the post-Neolithic Brassica napus
566 oilseed genome (vol 348, 1260782, 2014). *Science*, **345**, 1255–1255.

567 **Cheng, F., Mandáková, T., Wu, J., Xie, Q., Lysak, M.A. and Wang, X.** (2013)
568 Deciphering the diploid ancestral genome of the Mesohexaploid Brassica rapa. *Plant Cell*,
569 **25**, 1541–1554.

570 **Cheng, F., Wu, J., Fang, L. and Wang, X.** (2012) Syntenic gene analysis between Brassica
571 rapa and other Brassicaceae species. *Front. Plant Sci.*, **3**, 198.

572 **Clough, S.J. and Bent, A.F.** (1998) Floral dip: a simplified method for *Agrobacterium*-
573 mediated transformation of *Arabidopsis thaliana*. *Plant J.*, **16**, 735–743.

574 **Dobin, A., Davis, C.A., Schlesinger, F., Drenkow, J., Zaleski, C., Jha, S., Batut, P.,**
575 **Chaisson, M. and Gingeras, T.R.** (2013) STAR: ultrafast universal RNA-seq aligner.
576 *Bioinformatics*, **29**, 15–21.

577 **Endo, M., Yoshida, M., Sasaki, Y., et al.** (2018) Re-Evaluation of Florigen Transport
578 Kinetics with Separation of Functions by Mutations That Uncouple Flowering Initiation
579 and Long-Distance Transport. *Plant Cell Physiol.*, **59**, 1621–1629.

580 **Fernández, V., Takahashi, Y., Le Gourrierec, J. and Coupland, G.** (2016) Photoperiodic
581 and thermosensory pathways interact through CONSTANS to promote flowering at high
582 temperature under short days. *Plant J.*, **86**, 426–440.

583 **Fornara, F., Panigrahi, K.C.S., Gissot, L., Sauerbrunn, N., Rühl, M., Jarillo, J.A. and**
584 **Coupland, G.** (2009) Arabidopsis DOF transcription factors act redundantly to reduce

585 CONSTANS expression and are essential for a photoperiodic flowering response. *Dev.*
586 *Cell*, **17**, 75–86.

587 **Galvão, V.C., Fiorucci, A.-S., Trevisan, M., Franco-Zorilla, J.M., Goyal, A., Schmid-**
588 **Siegert, E., Solano, R. and Fankhauser, C.** (2019) PIF transcription factors link a
589 neighbor threat cue to accelerated reproduction in Arabidopsis. *Nat. Commun.*, **10**, 4005.

590 **Gnesutta, N., Kumimoto, R.W., Swain, S., Chiara, M., Siriwardana, C., Horner, D.S.,**
591 **Holt, B.F. and Mantovani, R.** (2017) CONSTANS Imparts DNA Sequence Specificity to
592 the Histone Fold NF-YB/NF-YC Dimer. *Plant Cell*, **29**, 1516–1532.

593 **Guo, Y., Hans, H., Christian, J. and Molina, C.** (2014) Mutations in single FT- and TFL1-
594 paralogs of rapeseed (Brassica napus L.) and their impact on flowering time and yield
595 components. *Front. Plant Sci.*, **5**, 282.

596 **Hatje, K., Keller, O., Hammesfahr, B., Pillmann, H., Waack, S. and Kollmar, M.** (2011)
597 Cross-species protein sequence and gene structure prediction with fine-tuned Webscipio 2.0
598 and Scipio. *BMC Res. Notes*, **4**, 265.

599 **Imaizumi, T., Schultz, T.F., Harmon, F.G., Ho, L.A. and Kay, S.A.** (2005) FKF1 F-box
600 protein mediates cyclic degradation of a repressor of CONSTANS in Arabidopsis. *Science*,
601 **309**, 293–297.

602 **Jaeger, K.E. and Wigge, P.A.** (2007) FT protein acts as a long-range signal in Arabidopsis.
603 *Curr. Biol.*, **17**, 1050–1054.

604 **Jang, S., Marchal, V., Panigrahi, K.C.S., Wenkel, S., Soppe, W., Deng, X.-W., Valverde,**
605 **F. and Coupland, G.** (2008) Arabidopsis COP1 shapes the temporal pattern of CO
606 accumulation conferring a photoperiodic flowering response. *EMBO J.*, **27**, 1277–1288.

607 **Jin, Q., Gao, G., Guo, C., et al.** (2022) Transposon insertions within alleles of BnaFT.A2 are
608 associated with seasonal crop type in rapeseed. *Theor. Appl. Genet.*, **135**, 3469–3483.

609 **Jin, Q., Yin, S., Li, G., et al.** (2021) Functional homoeologous alleles of CONSTANS
610 contribute to seasonal crop type in rapeseed. *Theor. Appl. Genet.*, **134**, 3287–3303.

611 **Jin, S., Nasim, Z., Susila, H. and Ahn, J.H.** (2021) Evolution and functional diversification
612 of FLOWERING LOCUS T/TERMINAL FLOWER 1 family genes in plants. *Semin. Cell*
613 *Dev. Biol.*, **109**, 20–30.

614 **Kagale, S., Robinson, S.J., Nixon, J., et al.** (2014) Polyploid evolution of the Brassicaceae
615 during the Cenozoic era. *Plant Cell*, **26**, 2777–2791.

616 **Kiełbasa, S.M., Wan, R., Sato, K., Horton, P. and Frith, M.C.** (2011) Adaptive seeds tame
617 genomic sequence comparison. *Genome Res.*, **21**, 487–493.

618 **Kim, S.-J., Hong, S.M., Yoo, S.J., Moon, S., Jung, H.S. and Ahn, J.H.** (2016) Post-
619 Translational Regulation of FLOWERING LOCUS T Protein in Arabidopsis. *Mol. Plant*,
620 **9**, 308–311.

621 **Kumar, S.V., Lucyshyn, D., Jaeger, K.E., Alós, E., Alvey, E., Harberd, N.P. and Wigge,**
622 **P.A.** (2012) Transcription factor PIF4 controls the thermosensory activation of flowering.
623 *Nature*, **484**, 242–245.

624 **Kumimoto, R.W., Adam, L., Hymus, G.J., Repetti, P.P., Reuber, T.L., Marion, C.M.,**
625 **Hempel, F.D. and Ratcliffe, O.J.** (2008) The Nuclear Factor Y subunits NF-YB2 and NF-
626 YB3 play additive roles in the promotion of flowering by inductive long-day photoperiods
627 in Arabidopsis. *Planta*, **228**, 709–723.

628 **Kumimoto, R.W., Zhang, Y., Siefers, N. and Holt, B.F.** (2010) NF-YC3, NF-YC4 and NF-
629 YC9 are required for CONSTANS-mediated, photoperiod-dependent flowering in
630 Arabidopsis thaliana. *Plant J.*, **63**, 379–391.

631 **Laubinger, S., Marchal, V., Le Gourrierec, J., et al.** (2006) Arabidopsis SPA proteins
632 regulate photoperiodic flowering and interact with the floral inducer CONSTANS to
633 regulate its stability. *Development*, **133**, 3213–3222.

634 **Liu, L., Adrian, J., Pankin, A., Hu, J., Dong, X., Korff, M. von and Turck, F.** (2014)
635 Induced and natural variation of promoter length modulates the photoperiodic response of
636 FLOWERING LOCUS T. *Nat. Commun.*, **5**, 4558.

637 **Liu, Y., Li, X., Li, K., Liu, H. and Lin, C.** (2013) Multiple bHLH proteins form
638 heterodimers to mediate CRY2-dependent regulation of flowering-time in Arabidopsis.
639 *PLoS Genet.*, **9**, e1003861.

640 **Liu, Y., Li, X., Ma, D., Chen, Z., Wang, J.-W. and Liu, H.** (2018) CIB1 and CO interact to
641 mediate CRY2-dependent regulation of flowering. *EMBO Rep.*, **19**.

642 **Li, B. and Dewey, C.N.** (2011) RSEM: accurate transcript quantification from RNA-Seq data
643 with or without a reference genome. *BMC Bioinformatics*, **12**, 323.

644 **Lu, K., Wei, L., Li, X., et al.** (2019) Whole-genome resequencing reveals Brassica napus
645 origin and genetic loci involved in its improvement. *Nat. Commun.*, **10**, 1154.

646 **Lv, X., Zeng, X., Hu, H., et al.** (2021) Structural insights into the multivalent binding of the
647 Arabidopsis FLOWERING LOCUS T promoter by the CO-NF-Y master transcription
648 factor complex. *Plant Cell*, **33**, 1182–1195.

649 **Panchy, N., Lehti-Shiu, M. and Shiu, S.-H.** (2016) Evolution of gene duplication in plants.
650 *Plant Physiol.*, **171**, 2294–2316.

651 **Parkin, I.A.P., Gulden, S.M., Sharpe, A.G., Lukens, L., Trick, M., Osborn, T.C. and**
652 **Lydiate, D.J.** (2005) Segmental structure of the Brassica napus genome based on
653 comparative analysis with Arabidopsis thaliana. *Genetics*, **171**, 765–781.

654 **Pin, P.A., Benlloch, R., Bonnet, D., Wremerth-Weich, E., Kraft, T., Gielen, J.J.L. and**
655 **Nilsson, O.** (2010) An antagonistic pair of FT homologs mediates the control of flowering
656 time in sugar beet. *Science*, **330**, 1397–1400.

657 **Posé, D., Verhage, L., Ott, F., Yant, L., Mathieu, J., Angenent, G.C., Immink, R.G.H.**
658 **and Schmid, M.** (2013) Temperature-dependent regulation of flowering by antagonistic
659 FLM variants. *Nature*, **503**, 414–417.

660 **Sawa, M., Nusinow, D.A., Kay, S.A. and Imaizumi, T.** (2007) FKF1 and GIGANTEA
661 complex formation is required for day-length measurement in Arabidopsis. *Science*, **318**,
662 261–265.

663 **Schiessl, S., Samans, B., Hüttel, B., Reinhard, R. and Snowdon, R.J.** (2014) Capturing
664 sequence variation among flowering-time regulatory gene homologs in the allopolyploid
665 crop species Brassica napus. *Front. Plant Sci.*, **5**, 404.

666 **Schiessl, S.** (2020) Regulation and Subfunctionalization of Flowering Time Genes in the
667 Allotetraploid Oil Crop Brassica napus. *Front. Plant Sci.*, **11**, 605155.

668 **Siriwardana, C.L., Gnesutta, N., Kumimoto, R.W., Jones, D.S., Myers, Z.A., Mantovani,**
669 **R. and Holt, B.F.** (2016) NUCLEAR FACTOR Y, Subunit A (NF-YA) Proteins Positively
670 Regulate Flowering and Act Through FLOWERING LOCUS T. *PLoS Genet.*, **12**,
671 e1006496.

672 **Song, J.-M., Guan, Z., Hu, J., et al.** (2020) Eight high-quality genomes reveal pan-genome
673 architecture and ecotype differentiation of Brassica napus. *Nat. Plants*, **6**, 34–45.

674 **Sparkes, I.A., Runions, J., Kearns, A. and Hawes, C.** (2006) Rapid, transient expression of
675 fluorescent fusion proteins in tobacco plants and generation of stably transformed plants.
676 *Nat. Protoc.*, **1**, 2019–2025.

677 **Takagi, H., Hempton, A.K. and Imaizumi, T.** (2023) Photoperiodic flowering in
678 Arabidopsis: Multilayered regulatory mechanisms of CONSTANS and the florigen
679 FLOWERING LOCUS T. *Plant Commun.*, **4**, 100552.

680 **Tamura, K., Stecher, G. and Kumar, S.** (2021) MEGA11: Molecular Evolutionary Genetics
681 Analysis version 11. *Mol. Biol. Evol.*, **38**, 3022–3027.

682 **Tang, H., Krishnakumar, V., Zeng, X., et al.** (2024) JCVI: A versatile toolkit for
683 comparative genomics analysis. *iMeta*, **3**, e211.

684 **Tang, H., Wang, X., Bowers, J.E., Ming, R., Alam, M. and Paterson, A.H.** (2008)
685 Unraveling ancient hexaploidy through multiply-aligned angiosperm gene maps. *Genome*
686 *Res.*, **18**, 1944–1954.

687 **Teotia, S. and Tang, G.** (2015) To bloom or not to bloom: role of microRNAs in plant
688 flowering. *Mol. Plant*, **8**, 359–377.

689 **Thaben, P.F. and Westermark, P.O.** (2014) Detecting rhythms in time series with RAIN. *J.*
690 *Biol. Rhythms*, **29**, 391–400.

691 **Tiwari, S.B., Shen, Y., Chang, H.-C., et al.** (2010) The flowering time regulator
692 CONSTANS is recruited to the FLOWERING LOCUS T promoter via a unique cis-
693 element. *New Phytol.*, **187**, 57–66.

694 **Valverde, F., Mouradov, A., Soppe, W., Ravenscroft, D., Samach, A. and Coupland, G.**
695 (2004) Photoreceptor regulation of CONSTANS protein in photoperiodic flowering.
696 *Science*, **303**, 1003–1006.

697 **Wang, J., Hopkins, C.J., Hou, J., Zou, X., Wang, C., Long, Y., Kurup, S., King, G.J. and**
698 **Meng, J.** (2012) Promoter variation and transcript divergence in Brassicaceae lineages of
699 FLOWERING LOCUS T. *PLoS ONE*, **7**, e47127.

700 **Wang, J., Long, Y., Wu, B., Liu, J., Jiang, C., Shi, L., Zhao, J., King, G.J. and Meng, J.**
701 (2009) The evolution of Brassica napus FLOWERING LOCUS T paralogues in the context
702 of inverted chromosomal duplication blocks. *BMC Evol. Biol.*, **9**, 271.

703 **Wang, Y., Tang, H., Debarry, J.D., et al.** (2012) MCScanX: a toolkit for detection and
704 evolutionary analysis of gene synteny and collinearity. *Nucleic Acids Res.*, **40**, e49.

705 **Wenkel, S., Turck, F., Singer, K., Gissot, L., Le Gourrierec, J., Samach, A. and**
706 **Coupland, G.** (2006) CONSTANS and the CCAAT box binding complex share a
707 functionally important domain and interact to regulate flowering of Arabidopsis. *Plant Cell*,
708 **18**, 2971–2984.

709 **Wigge, P.A., Kim, M.C., Jaeger, K.E., Busch, W., Schmid, M., Lohmann, J.U. and**
710 **Weigel, D.** (2005) Integration of spatial and temporal information during floral induction in
711 Arabidopsis. *Science*, **309**, 1056–1059.

712 **Wu, D., Liang, Z., Yan, T., et al.** (2019) Whole-Genome Resequencing of a Worldwide
713 Collection of Rapeseed Accessions Reveals the Genetic Basis of Ecotype Divergence. *Mol.*
714 *Plant*, **12**, 30–43.

715 **Yamaguchi, A., Kobayashi, Y., Goto, K., Abe, M. and Araki, T.** (2005) TWIN SISTER
716 OF FT (TSF) acts as a floral pathway integrator redundantly with FT. *Plant Cell Physiol.*,
717 **46**, 1175–1189.

718 **Yanovsky, M.J. and Kay, S.A.** (2002) Molecular basis of seasonal time measurement in
719 Arabidopsis. *Nature*, **419**, 308–312.

720 **Yoo, S.-C., Chen, C., Rojas, M., Daimon, Y., Ham, B.-K., Araki, T. and Lucas, W.J.**
721 (2013) Phloem long-distance delivery of FLOWERING LOCUS T (FT) to the apex. *Plant*
722 *J.*, **75**, 456–468.

723 **Zicola, J., Liu, L., Tänzler, P. and Turck, F.** (2019) Targeted DNA methylation represses
724 two enhancers of FLOWERING LOCUS T in Arabidopsis thaliana. *Nat. Plants*, **5**, 300–
725 307.

726 **Zou, J., Mao, L., Qiu, J., et al.** (2019) Genome-wide selection footprints and deleterious
727 variations in young Asian allotetraploid rapeseed. *Plant Biotechnol. J.*, **17**, 1998–2010.

728

729 # Figure legends

730 **Figure 1. Phylogenetic and syntenic analysis of *FT* and *TSF* and their homologues in *B.***
731 ***napus*, *B. oleracea* and *S. parvula*.** (A)-(D) Microsynteny between *FT* homologs. *FT*-like
732 genes from *A. thaliana* (bottom), *S. parvula* (middle) and *B. napus* (top) are connected by red
733 lines, orthologs of flanking genes present in all genomes are connected by golden lines,
734 orthologs of flanking genes that exist only in a subset of Brassica genomes are connected by
735 purple, blue and gray lines. Genes are depicted as boxes (blue forward, green reverse
736 orientation). **(A)** Four paralogous *FT* orthologs were identified in *B. napus*, one in *S. parvula*.
737 **(B)** One *TSF* ortholog was identified in *S. parvula*, none in *B. napus*. **(C)** Three paralogous *FT*-
738 like genes (*BnaNFT*) on Chr. A07/C02/C06 in *B. napus* have an ortholog in *S. parvula*, but not
739 in *A. thaliana*. Only the paralogue on chromosome A07 (*BnaNFT.A7*) encodes a functional
740 gene. **(D)** An *FT*-like gene on Chr. C04 (*BnaCFT.C4*) in *B. napus*, is present in the C-genome
741 parent *B. oleracea* and absent in the *S. parvula* and *A. thaliana* genomes. (**E)** Full-length protein
742 sequences of FT, TSF and FT homologues obtained by blast analysis against *B. napus*, *B. rapa*,
743 *B. oleracea, A. lyrata* and *S. parvula* genomes were used to create the neighbour-joining (NJ)
744 consensus tree using MEGA-11 with 1,000 bootstraps. TFL1, BFT, MFT were set as an
745 outgroup, and FT and TSF orthologues in *A. thaliana* and *A. lyrata* were added for reference.

746 **Figure 2. Florigen function of *B. napus FT* homologs. (A)** Scheme of expression cassettes
747 used for complementation test. **(B)** Flowering time as total leaf number of T3 plants of two
748 representative *ft-10* lines transformed with *FT* and *B. napus FT* homologs driven by *(C+A)-*
749 *FTp*. The number of plants used for analysis is indicated above the x-axis. **(C)** Flowering time
750 of independent T1 *ft-10* plants transformed with *FT* and *B. napus FT* homologs under the
751 control of *FD*p. The number of independent T1 plants used for analysis is indicated above the
752 x-axis. **(D)** Selection of amino-acids alignment of *A. thaliana* and *B. napus FT* homologs.
753 Arrows indicate differences between *BnaFT.A7* and *BnaFT.C6*. *BnaFT.A7m* and *BnaFT.C6m*
754 are mutant versions in which the last amino acid residue was swapped. **(E)** Flowering time of
755 independent T1 *ft-10* T1 plants transformed with *BnaFT.C6, BnaFT.A7, BnaFTC6m and*
756 *BnaFTA7m* driven by *(C+A)-FTp*. T The number of independent T1 plants used for analysis is
757 indicated above the x-axis. (A, B, D) Flowering time was scored as total leaf number. Box plots
758 show the medians as vertical lines; box limits indicate the 25th and 75th percentiles. Different
759 symbols from a to h above the plots indicate significant differences ($P < 0.05$, two-way analysis
760 of variance (ANOVA) with Tukey's multiple comparison test).

761 **Figure 3. Tissue-specific expression of *B. napus FT* homologs in ZS11.** Expression of *B.*
762 *napus FT* homologs in roots, leaf 6, leaf 8, paraclade leaf, floral bud, flower and siliques. Plants
763 were sown in the greenhouse for 4 weeks under LD conditions, then vernalized for 4 weeks
764 before being transferred back to LD conditions in the greenhouse. Root and leaf 6 and 8 were
765 sampled before vernalization, leaf 8, paraclade leaf, floral bud, flower and siliques were
766 sampled after vernalization at ZT12. Boxes represent inner quartiles of three biological
767 replicates, medians are indicated by vertical lines, single measurements are indicated by dots.
768 *BnaENTH* was used as reference gene, all values were compared to genomic DNA, which was
769 set as 1.

770 **Figure 4. Conservation of the cis-regulatory code at *B. napus FT* homologs.**
771 Schematic diagram showing the distribution of motifs within conserved blocks A **(A)**, C **(B)**
772 and E **(C)** for *FT-like* genes from *A. thaliana, S. parvula* and *B. napus*. Gray boxes indicate
773 aligned sequences, white spaces indicate alignment gaps. Cis-elements are marked in different
774 colors as indicated in the common legend. The length of the unaligned sequences is shown after
775 each alignment block. Red numbers above the position of motifs at *FT* block A indicate
776 previously characterized functional motifs. (**D)** Scheme of the promoter region of *B. napus FT*
777 genes fused to LUC68. (**E)** Promoter-reporter transactivation assay in infiltrated tobacco leaves.
778 Agrobacteria transformed with a binary vector containing promoter Firefly green shifted
779 luciferase fusions were co-infiltrated with cultures expressing red shifted luciferase and either
780 CO, BnaCO.A10, BnaCO.C9 or H2B under the control of the CaMV 35S promoter. Luciferase
781 activity was detected with the help of a CCD camera through selective filters. Boxplots show
782 relative green versus red luciferase signal after filter leakage correction from 4 to 6 independent
783 infiltrations of three different leaves, the median is indicated as line, data-points as dots.
784 Statistical analysis was performed using the non-parametric Wilcocxon signed rank test with
785 FDR correction.

786 **Figure 5. Diurnal expression of *B.* napus *FT* and *CO* homologs in ZS11. (A)** Diurnal
787 expression of *BnaFT.A2*, *BnaFT.C2*, *BnaFT.A7*, *BnaFT.C6*. **(B)** Diurnal expression of
788 *BnaNFT.A7* and *BnaCFT.C4.* (**C)** Diurnal expression of *BnaCO.A10* and *BnaCO.C9.* Material
789 from leaf 6 and leaf 8 were sampled every 4 h from ZS11 plants grown in SD and LD
790 photoperiod in growth chambers at 22°C before (BV) and after (AV) vernalization,
791 respectively. Time is plotted in reference to Zeitgeber (light on). Expression levels were
792 analysed by gene-specific qRT-PCR using four independent biological replicates using
793 genomic DNA as common reference point. *BnaENTH* was used to correct for differences in
794 cDNA amount. Values for ZT0 and ZT24 were pooled at both time points. Data points are

795 indicated as dots, lines were generated using a loess smoothing function, grey shapes indicate
796 ± standard error.

797 **Figure 6. Diurnal expression of *B.* napus NF-Y homologs. (A)** Venn diagram showing
798 rhythmically expressed genes in LD and SD photoperiod. (**B)** As A) for NF-Y genes. **(C)**
799 Heatmap of rhythmically expressed *B. napus* NF-Y genes after hierarchical clustering based on
800 expression patterns. Expression data in TPM were normalized across all samples per gene,
801 clustering was performed using the Manhattan distance metric. Colours indicate *B. napus*
802 homologs of *NF-Y*s involved in *FT* regulation (red), *BnaFT*s (blue) and *BnaCO*s (purple). (**D)**
803 Cumulative sum plot of TPM values in SD (left panel) and LD (right panel) for all *BnaNFYB2*
804 genes. (**E)** as D) for *BnaNF-YC9* genes. (**F)** as D) for *BnaNF-YA2* genes.

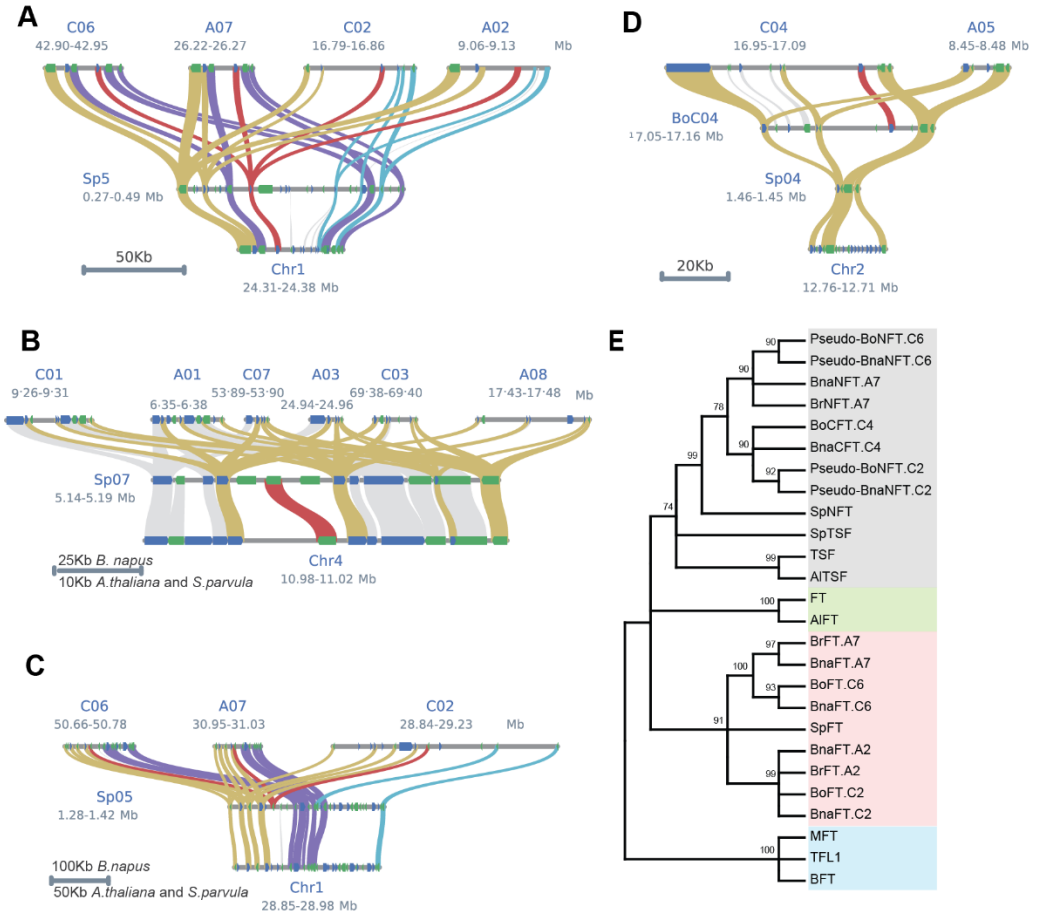

Figure 1. Phylogenetic and syntenic analysis of *FT* and *TSF* and their homologues in *B. napus*, *B. oleracea* and *S. parvula*. (A)-(D) Microsynteny between *FT* homologs. *FT*-like genes from *A. thaliana* (bottom), *S. parvula* (middle) and *B. napus* (top) are connected by red lines, orthologs of flanking genes present in all genomes are connected by golden lines, orthologs of flanking genes that exist only in a subset of Brassica genomes are connected by purple, blue and gray lines. Genes are depicted as boxes (blue forward, green reverse orientation). **(A)** Four paralogous *FT* orthologs were identified in *B. napus*, one in *S. parvula*. **(B)** One *TSF* ortholog was identified in *S. parvula*, none in *B. napus*. **(C)** Three paralogous *FT*-like genes (*BnaNFT*) on Chr. A07/C02/C06 in *B. napus* have an ortholog in *S. parvula*, but not in *A. thaliana*. Only the paralogue on chromosome A07 (*BnaNFT.A7*) encodes a functional gene. **(D)** An *FT*-like gene on Chr. C04 (*BnaCFT.C4*) in *B. napus*, is present in the C-genome parent *B. oleracea* and absent in the *S. parvula* and *A. thaliana* genomes. **(E)** Full-length protein sequences of FT, TSF and FT homologues obtained by blast analysis against *B. napus*, *B. rapa*, *B. oleracea, A. lyrata* and *S. parvula* genomes were used to create the neighbour-joining (NJ) consensus tree using MEGA-11 with 1,000 bootstraps. TFL1, BFT, MFT were set as an outgroup, and FT and TSF orthologues in *A. thaliana* and *A. lyrata* were added for reference.

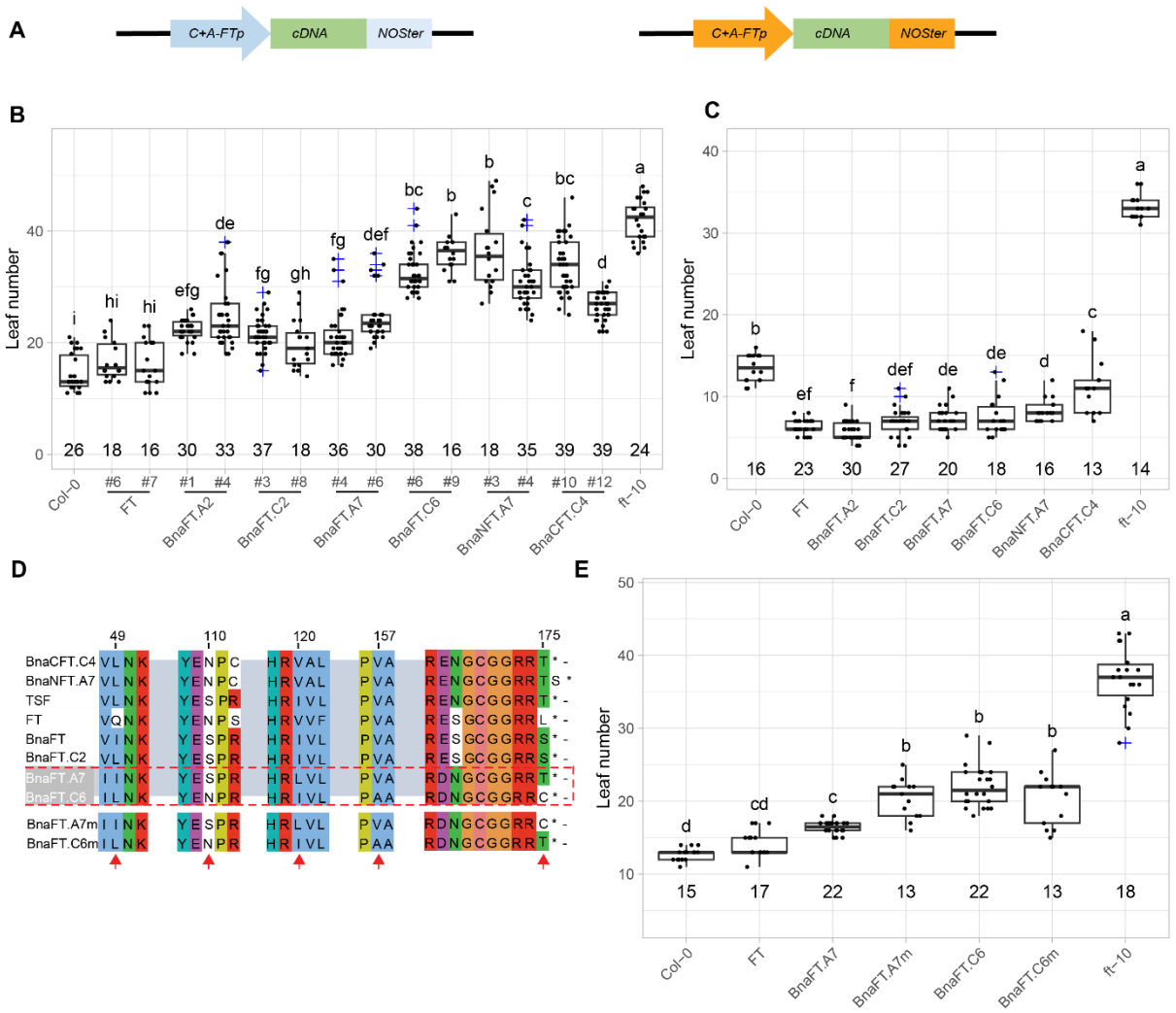

Figure 2. Florigen function of *B. napus FT* homologs. (A) Scheme of expression cassettes used for complementation test. **(B)** Flowering time as total leaf number of T3 plants of two representative *ft-10* lines transformed with *FT* and *B. napus FT* homologs driven by *(C+A)-FTp*. The number of plants used for analysis is indicated above the x-axis. **(C)** Flowering time of independent T1 *ft-10* plants transformed with *FT* and *B. napus FT* homologs under the control of *FD*p. The number of independent T1 plants used for analysis is indicated above the x-axis. **(D)** Selection of amino-acids alignment of *A. thaliana* and *B. napus FT* homologs. Arrows indicate differences between *BnaFT.A7* and *BnaFT.C6*. *BnaFT.A7m* and *BnaFT.C6m* are mutant versions in which the last amino acid residue was swapped. **(E)** Flowering time of independent T1 *ft-10* T1 plants transformed with *BnaFT.C6, BnaFT.A7, BnaFTC6m and BnaFTA7m* driven by *(C+A)-FTp*. T The number of independent T1 plants used for analysis is indicated above the x-axis. (A, B, D) Flowering time was scored as total leaf number. Box plots show the medians as vertical lines; box limits indicate the 25th and 75th percentiles, blue crosses mark outliers. Different symbols from a to h above the plots indicate significant differences ($P < 0.05$, two-way analysis of variance (ANOVA) with Tukey's multiple comparison test).

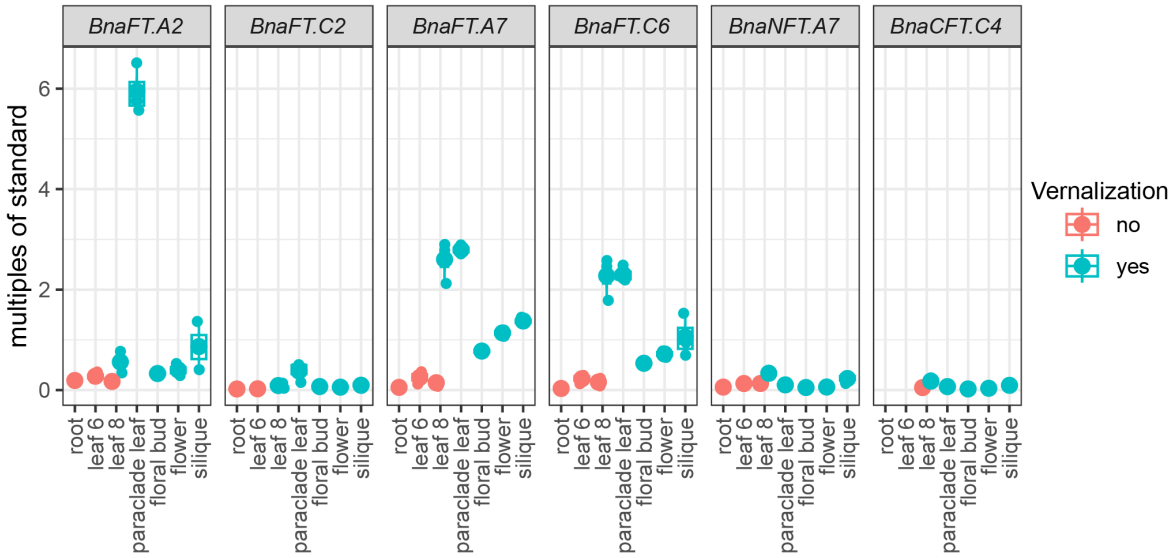

Figure 3. Tissue-specific expression of *B. napus FT* homologs in ZS11. Expression of *B. napus FT* homologs in roots, leaf 6, leaf 8, paraclade leaf, floral bud, flower and siliques. Plants were sown in the greenhouse for 4 weeks under LD conditions, then vernalized for 4 weeks before being transferred back to LD conditions in the greenhouse. Root and leaf 6 and 8 were sampled before vernalization, leaf 8, paraclade leaf, floral bud, flower and siliques were sampled after vernalization at ZT12. Boxes represent inner quartiles of three biological replicates, medians are indicated by vertical lines, single measurements are indicated by dots. *BnaENTH* was used as reference gene, all values were compared to genomic DNA, which was set as 1.

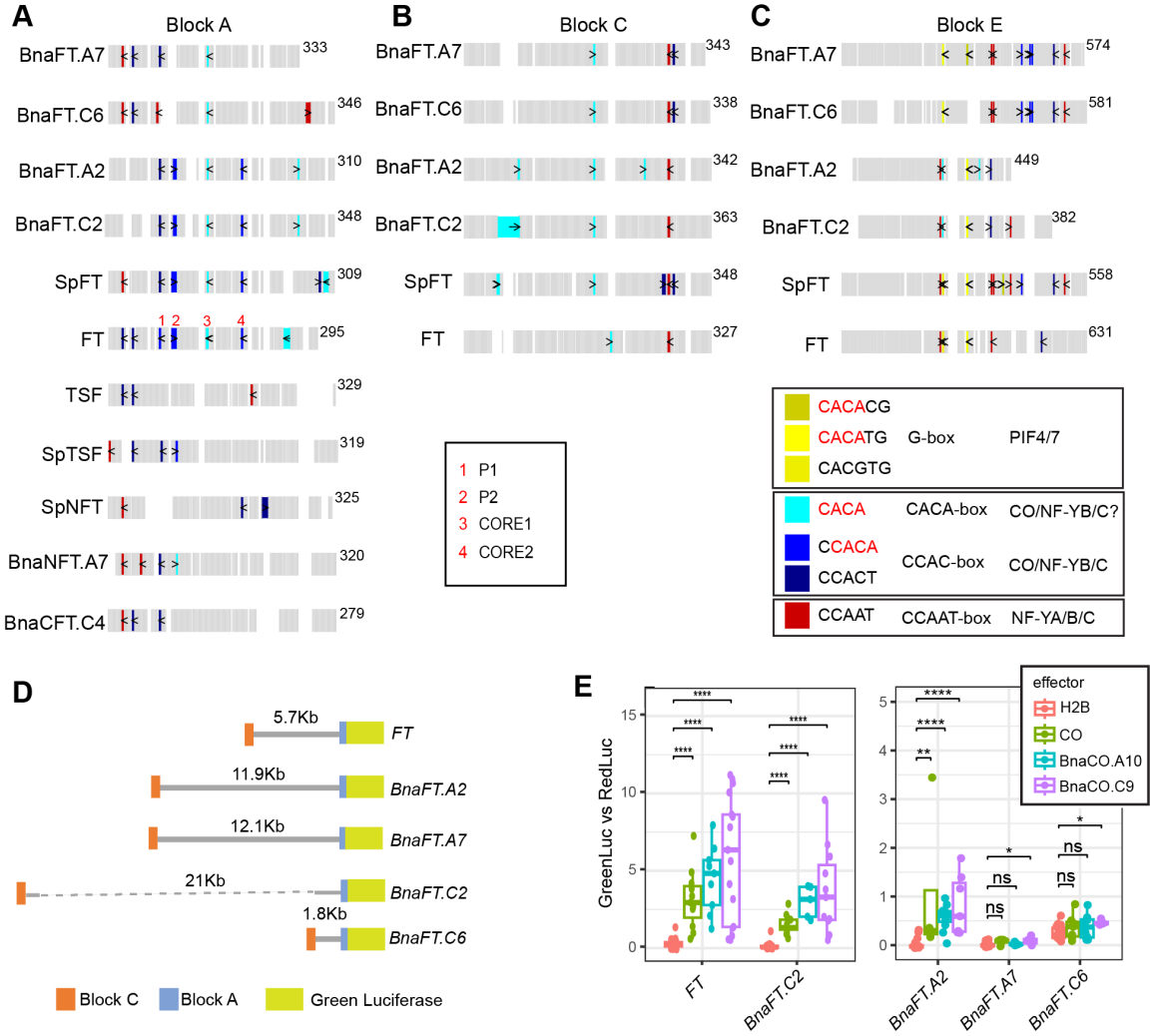

Figure 4. Conservation of the cis-regulatory code at *B. napus FT* homologs.
Schematic diagram showing the distribution of motifs within conserved blocks A **(A)**, C **(B)** and E **(C)** for *FT-like* genes from *A. thaliana, S. parvula* and *B. napus*. Gray boxes indicate aligned sequences, white spaces indicate alignment gaps. Cis-elements are marked in different colors as indicated in the common legend. The length of the unaligned sequences is shown after each alignment block. Red numbers above the position of motifs at *FT* block A indicate previously characterized functional motifs. **(D)** Scheme of the promoter region of *B. napus FT* genes fused to LUC68. **(E)** Promoter-reporter transactivation assay in infiltrated tobacco leaves. Agrobacteria transformed with a binary vector containing promoter Firefly green shifted luciferase fusions were co-infiltrated with cultures expressing red shifted luciferase and either CO, BnaCO.A10, BnaCO.C9 or H2B under the control of the CaMV 35S promoter. Luciferase activity was detected with the help of a CCD camera through selective filters. Boxplots show relative green versus red luciferase signal after filter leakage correction from 4 to 6 independent infiltrations of three different leaves, the median is indicated as line, data-points as dots. Statistical analysis was performed using the non-parametric Wilcocxon signed rank test with FDR correction.

870

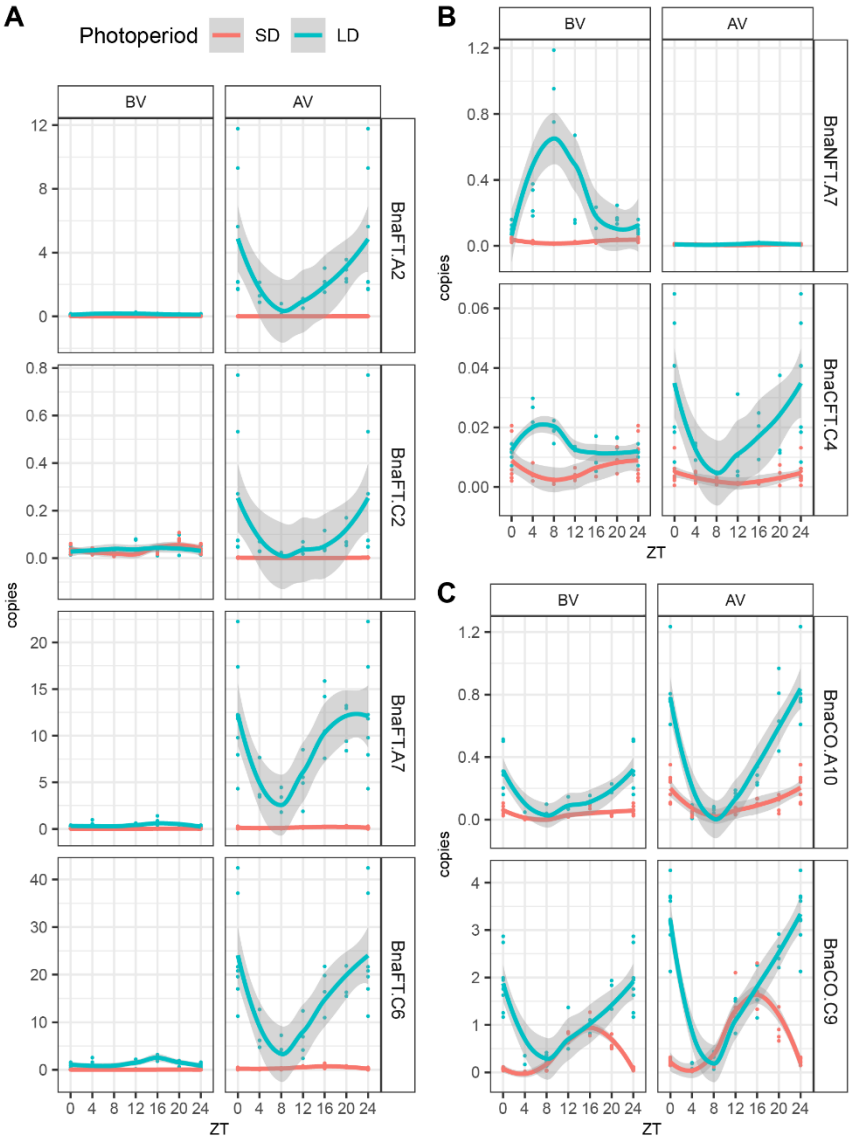

871

872 **Figure 5. Diurnal expression of *B. napus* *FT* and *CO* homologs in ZS11. (A)** Diurnal
873 expression of *BnaFT.A2*, *BnaFT.C2*, *BnaFT.A7*, *BnaFT.C6*. **(B)** Diurnal expression of
874 *BnaNFT.A7* and *BnaCFT.C4*. **(C)** Diurnal expression of *BnaCO.A10* and *BnaCO.C9*. Material
875 from leaf 6 and leaf 8 were sampled every 4 h from ZS11 plants grown in SD and LD
876 photoperiod in growth chambers at 22°C before (BV) and after (AV) vernalization,
877 respectively. Time is plotted in reference to Zeitgeber (light on). Expression levels were
878 analysed by gene-specific qRT-PCR using four independent biological replicates using
879 genomic DNA as common reference point. *BnaENTH* was used to correct for differences in
880 cDNA amount. Values for ZT0 and ZT24 were pooled at both time points. Data points are
881 indicated as dots, lines were generated using a loess smoothing function, grey shapes indicate
882 ± standard error.

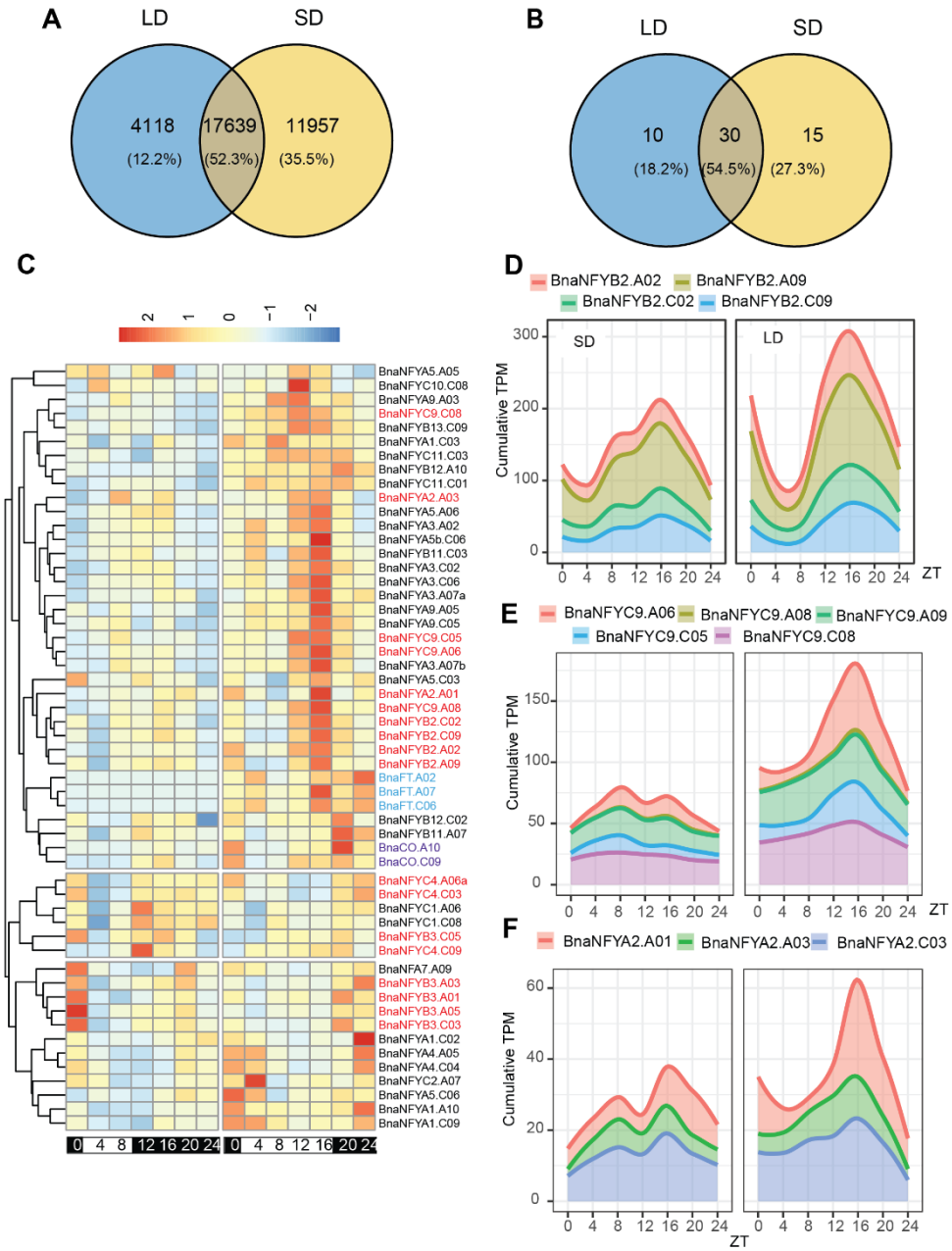

Figure 6. Diurnal expression of *B. napus* NF-Y homologs. (A) Venn diagram showing rhythmically expressed genes in LD and SD photoperiod. **(B)** As A) for NF-Y genes. **(C)** Heatmap of rhythmically expressed *B. napus* NF-Y genes after hierarchical clustering based on expression patterns. Expression data in TPM were normalized across all samples per gene, clustering was performed using the Manhattan distance metric. Colours indicate *B. napus* homologs of *NF-Y*s involved in *FT* regulation (red), *BnaFT*s (blue) and *BnaCO*s (purple). **(D)** Cumulative sum plot of TPM values in SD (left panel) and LD (right panel) for all *BnaNFYB2* genes. **(E)** as D) for *BnaNF-YC9* genes. **(F)** as D) for *BnaNF-YA2* genes.